

See discussions, stats, and author profiles for this publication at: <https://www.researchgate.net/publication/24270218>

Electrochemical and Electrogenenerated Chemiluminescent Studies of a Trinuclear Complex, $[(\text{phen})_2\text{Ru}(\text{dpp})_2\text{RhCl}_2]^{5+}$, and Its Interactions with Calf Thymus DNA

ARTICLE in ANALYTICAL CHEMISTRY · MAY 2009

Impact Factor: 5.64 · DOI: 10.1021/ac900282y · Source: PubMed

CITATIONS

23

READS

22

10 AUTHORS, INCLUDING:



Shijun Wang

Drexel University

12 PUBLICATIONS 157 CITATIONS

SEE PROFILE



Varma H Rambaran

The University of Trinidad and Tobago

8 PUBLICATIONS 30 CITATIONS

SEE PROFILE



Alvin Holder

Old Dominion University

57 PUBLICATIONS 472 CITATIONS

SEE PROFILE

Electrochemical and Electrogenenerated Chemiluminescent Studies of a Trinuclear Complex, $[((\text{phen})_2\text{Ru}(\text{dpp}))_2\text{RhCl}_2]^{5+}$, and Its Interactions with Calf Thymus DNA

Shijun Wang,[†] Jenifer Milam,[†] André C. Ohlin,[†] Varma H. Rambaran,[‡] Eva Clark,[†] Woodrow Ward,[†] Luke Seymour,[†] William H. Casey,[†] Alvin A. Holder,[†] and Wujian Miao^{*,†}

Department of Chemistry and Biochemistry, The University of Southern Mississippi, Hattiesburg, Mississippi 39406, and Department of Chemistry, The University of Trinidad and Tobago, Trinidad and Tobago

The electrochemical behavior of a trinuclear ruthenium(II)-containing complex, $[((\text{phen})_2\text{Ru}(\text{dpp}))_2\text{RhCl}_2]^{5+}$ (where phen = 1,10-phenanthroline, dpp = 2,3-bis(2-pyridyl)pyrazine), was studied in acetonitrile (MeCN) and aqueous solutions. In MeCN containing 0.10 M tetra-*n*-butylammonium perchlorate (TBAP), the complex displayed a reversible, overlapping $\text{Ru}^{\text{II/III}}$ redox process with $E_{1/2} = +1.21$ V vs Ag/Ag^+ (10 mM), an irreversible reduction of $\text{Rh}^{\text{III/II}}$ at -0.73 V vs Ag/Ag^+ , and two quasi-reversible dpp/dpp[−] couples with $E_{1/2} = -1.11$ and -1.36 V vs Ag/Ag^+ at a Pt electrode with a scan rate of 50 mV s^{−1}. In 0.20 M Tris buffer solution (pH 7.4), an irreversible, overlapping $\text{Ru}^{\text{II/III}}$ oxidation at $+1.48$ V vs Ag/AgCl (3 M KCl), and an irreversible reduction of $\text{Rh}^{\text{III/II}}$ at -0.78 V vs Ag/AgCl were observed at a glassy carbon electrode with a scan rate of 50 mV/s. Investigations on the electrogenerated chemiluminescence (ECL) of the complex revealed that 2-(dibutylamino) ethanol (DBAE) was superior to tri-*n*-propylamine (TPrA) as an ECL coreactant within their entire concentration range of 10–100 mM in MeCN, and in aqueous media, as low as 1.0 nM of the complex can be detected using TPrA coreactant ECL. A maximum ECL emission of 640 nm, which is about 55 nm blue shift to its fluorescence, was observed in MeCN with DBAE as a coreactant. Interactions of the complex with calf thymus DNA (ctDNA) were conducted with a flow-cell based quartz-crystal microbalance, and a binding constant of $2.5 \times 10^5 \text{ M}^{-1}$ was calculated on the basis of the Langmuir isotherm equation.

Electrogenenerated chemiluminescence (ECL), a process of light generation initiated by electrochemical reactions, has proven to be a very powerful analytical technique and been widely used in the areas of, for example, DNA probe, immunoassay, biowarfare agent testing, and environmental detection, because of its inherent

features such as low background, high sensitivity, and excellent selectivity.^{1–4} These applications are predominantly based on the fundamental ECL research work of a variety of inorganic and organic compounds^{1,2,5} as well as different types of nanomaterials⁶ including semiconductive quantum dots⁷ over the past 45 years since the pioneering ECL studies reported by Kuwana, Hercules, and Bard et al.^{8–11} in the mid-1960s. Although ECL can be produced via ion annihilation reactions, which generally require the experiments conducted in dried organic solvent in the absence of molecular oxygen so that a wide potential window (both in positive and in negative directions) can be obtained and the ECL quenching by oxygen can be eliminated,¹² the majority of the ECL applications have been performed in aqueous media via the oxidative-reduction type coreactant ECL reactions¹³ involving tris(2,2'-bipyridine)ruthenium(II) cation ($\text{Ru}(\text{bpy})_3^{2+}$) or its derivatives as luminophore species and tri-*n*-propylamine (TPrA) or its analogues as the coreactant.¹⁴ This type of coreactant ECL needs the potential scanning or pulsing only in the positive region, and the atmosphere effect (i.e., moisture and oxygen) on the ECL production is insignificant under commonly used experimental conditions. As a result, ECL-based detectors have been successfully incorporated into many analytical detection systems, which include flow injection analysis, high-performance liquid chromatography, capillary electrophoresis, and

- (1) Miao, W. *Chem. Rev.* **2008**, *108*, 2506–2553.
- (2) Richter, M. M. *Chem. Rev.* **2004**, *104*, 3003–3036.
- (3) *Electrogenenerated Chemiluminescence*; Bard, A. J., Ed.; Marcel Dekker, Inc.: New York, 2004.
- (4) Xu, X.-H. N.; Zu, Y. In *New Frontiers in Ultrasensitive Bioanalysis*; Xu, X.-H. N., Ed.; John Wiley & Sons, Inc.: Hoboken, NJ, 2007; Vol. 172, pp 235–267.
- (5) Richter, M. M. In *Electrogenenerated Chemiluminescence*; Bard Allen, J., Ed.; Marcel Dekker, Inc.: New York, 2004, pp 321–358, Chapter 7.
- (6) Qi, H.; Peng, Y.; Gao, Q.; Zhang, C. *Sensors* **2009**, *9*, 674–695.
- (7) Bard, A. J.; Ding, Z.; Myung, N. *Structure and Bonding (Berlin, Germany)* **2005**, *118*, 1–57.
- (8) Kuwana, T.; Epstein, B.; Seo, E. T. *J. Phys. Chem.* **1963**, *67*, 2243–2244.
- (9) Santhanam, K. S. V.; Bard, A. J. *J. Am. Chem. Soc.* **1965**, *87*, 139–140.
- (10) Hercules, D. M. *Science* **1964**, *145*, 808.
- (11) Visco, R. E.; Chandross, E. A. *J. Am. Chem. Soc.* **1964**, *86*, 5350.
- (12) Fan, F. R. F. In *Electrogenenerated Chemiluminescence*; Bard, A. J., Ed.; Marcel Dekker, Inc.: New York, 2004, pp 23–100, Chapter 2.
- (13) Rubinstein, I.; Bard, A. J. *J. Am. Chem. Soc.* **1981**, *103*, 512–516.
- (14) Miao, W.; Choi, J.-P. In *Electrogenenerated Chemiluminescence*; Bard, A. J., Ed.; Marcel Dekker, Inc.: New York, 2004; Chapter 5, pp 213–272.

* To whom correspondence should be addressed. E-mail: wujian.miao@usm.edu. Phone: +1 601-266 4716. Fax: +1 601-266 6075.

[†] The University of Southern Mississippi.

[‡] The University of Trinidad and Tobago.

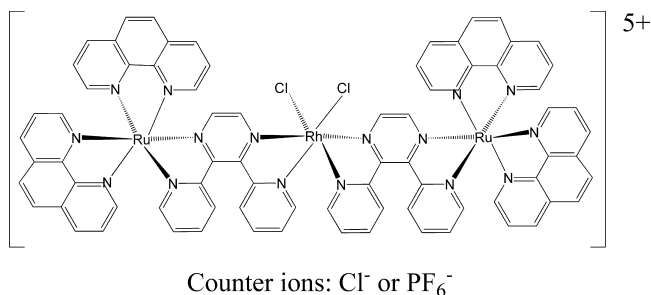


Figure 1. Structure of $[(\text{phen})_2\text{Ru}(\text{dpp})]_2\text{RhCl}_2]^{5+}$.

micro total analysis, for the quantification of analytes that could act as either ECL emitters or ECL coreactants.^{15,16}

Among a large number of inorganic and organometallic complexes studied, only several reports on ECL with multimetallic systems have appeared, which include Mo,^{17–19} W,^{19,20} Pt,^{21–23} and Pb²⁴ clusters, as well as bimetallic Ru complexes.^{25,26} Most of their ECL experiments were conducted in organic or mixed media because of the insolubility and instability of these complexes in an aqueous environment. In contrast to the metallic clusters, where weak ECL emissions were generally observed, bimetallic Ru complexes have demonstrated several times increases in ECL efficiency with respect to the Ru(bpy)₃²⁺ standard,^{25,26} making them promising ECL labels for use in analytical applications.

In the present study, the electrochemical and ECL behavior of a trinuclear, mixed-metal supramolecular complex, $[(\text{phen})_2\text{Ru}(\text{dpp})]_2\text{RhCl}_2]^{5+}$ (where phen = 1,10-phenanthroline, dpp = 2,3-bis(2-pyridyl)pyrazine, Figure 1), is reported. This complex, like other trinuclear complexes coupling light-absorbing ruthenium centers to reactive metal centers (e.g., $[(\text{bpy})_2\text{Ru}(\text{BL})]_2\text{MCl}_2]^{5+}$, where M = Rh^{III} or Ir^{III} and BL = dpp²⁷ or 2,2'-bipyrimidine²⁸), could offer the ability to control spectroscopic and redox properties important to photochemical applications. Recently, $[(\text{bpy})_2\text{Ru}(\text{dpp})]_2\text{RhCl}_2](\text{PF}_6)_5$ complex has demonstrated the ability to produce H₂ when excited with visible light in acetonitrile/H₂O solution in the presence of dimethylaniline electron donor.²⁹ Moreover, the photocleaving of DNA and the

photochemical inhibition of cell replication of this complex^{30,31} suggest strong interactions of the complex with DNA. Therefore, another objective of this study is to quantitatively monitor the intercalations of $[(\text{phen})_2\text{Ru}(\text{dpp})]_2\text{RhCl}_2]^{5+}$ complex into DNA and to estimate the binding constant of the interactions using a quartz crystal microbalance (QCM). This is the very first report of the binding kinetics involving trinuclear Ru–Rh complex and calf thymus DNA through the use of QCM.

EXPERIMENTAL SECTION

Chemicals and Materials. Tri-*n*-propylamine (TPA, 99+%), sulfuric acid (H₂SO₄, 98%), nitric acid (HNO₃, 70%), and 11-mercapto-1-undecanol [HSCH₂(CH₂)₉CH₂OH, 97%] from Aldrich (Milwaukee, WI), hydrochloric acid (HCl, 37.5%), hydrogen peroxide (H₂O₂, 30%), and sodium chloride (NaCl, certified A.C.S.) from Fisher (Fairlawn, NJ), sodium hydroxide (NaOH, 98.7%) from J. T. Baker (Phillipsburg, NJ), silver nitrate (AgNO₃, 99.5%), and tetrabutylammonium perchlorate (TBAP, 99+%, electrochemical grade) from Fluka (Milwaukee, WI), acetonitrile (MeCN, 99.93+%, HPLC grade), 2-(dibutylamino)-ethanol (DBAE, 99%), calf thymus DNA (ctDNA), and 2-morpholinoethanesulfonic acid (MES, 99+%) from Sigma (St. Louis, MO), and 1-ethyl-3-(3-dimethylaminopropyl) carbodiimide (EDAC) and tris(hydroxymethyl)-aminomethane (Tris) from Pierce (Rockford, IL) were used as received. All aqueous solutions were prepared with deionized–distilled water produced from a Barnstead MP-6A Mega-Pure system (Barnstead international Dubuque, Iowa).

Synthesis of $[(\text{phen})_2\text{Ru}(\text{dpp})]_2\text{RhCl}_2]^{5+}$ Complexes. Water insoluble $[(\text{phen})_2\text{Ru}(\text{dpp})]_2\text{RhCl}_2](\text{PF}_6)_5$ and water-soluble $[(\text{phen})_2\text{Ru}(\text{dpp})]_2\text{RhCl}_2]\text{Cl}_5$ complexes were synthesized using procedures similar to those previously reported,^{27,31} and characterized by UV–visible spectroscopy and ESI mass spectroscopy (see Supporting Information section for details).

Instrumentation. Cyclic voltammetry (CV) was carried out with a model 660A electrochemical workstation (CH Instruments, Austin, TX). A conventional three-electrode cell was used, with a Pt wire as the counter electrode and an Ag/AgCl/Cl⁻ (3.0 M KCl) or Ag/Ag⁺ (10 mM AgNO₃ and 0.10 M TBAP in MeCN) as the reference electrode. Three different types of working electrodes, namely glassy carbon (GC, 3 mm diameter), Pt (2 mm diameter), and gold (Au, 2 mm diameter), were used for CV and ECL measurements. These electrodes were polished with 0.3–0.05 μm alumina slurry, thoroughly rinsed with water, and dried with the Kim wipes facial tissue before each experiment. The electrolyte solution was purged with high purity nitrogen (Nordan Smith, Hattiesburg, MS) for ~10 min and kept under nitrogen atmosphere during the measurement whenever a negative potential range was used.

The ECL signals along with the CV responses were measured simultaneously with a homemade ECL instrument as described previously.^{32,33} This instrument combined the 660A electrochemical workstation with a photomultiplier tube (PMT, Hamamatsu R928, Japan) biased at a voltage of –700 V via a high voltage power supply (Model 472A Brandenburg PMT power supply, England),

- (15) Yin, X.-B.; Dong, S.; Wang, E. *TrAC, Trends Anal. Chem.* **2004**, *23*, 432–441.
- (16) Danielson, N. D. In *Electrogenerated Chemiluminescence*; Bard, A. J., Ed.; Marcel Dekker, Inc.: New York, 2004; Chapter 9, pp 397–444.
- (17) Ouyang, J.; Zietlow, T. C.; Hopkins, M. D.; Fant, F. R. F.; Gray, H. B.; Bard, A. J. *J. Phys. Chem.* **1986**, *90*, 3841–3844.
- (18) Maverick, A. W.; Gray, H. B. *J. Am. Chem. Soc.* **1981**, *103*, 1298–1300.
- (19) Maverick, A. W.; Najdzionek, J. S.; MacKenzie, D.; Nocera, D. G.; Gray, H. B. *J. Am. Chem. Soc.* **1983**, *105*, 1878–1882.
- (20) Mussell, R. D.; Nocera, D. G. *Inorg. Chem.* **1990**, *29*, 3711–3717.
- (21) Vogler, A.; Kunkely, H. *Angew. Chem.* **1984**, *96*, 299–300.
- (22) Kim, J.; Fan, F. F.; Bard, A. J.; Che, C. M.; Gray, H. B. *Chem. Phys. Lett.* **1985**, *121*, 543–546.
- (23) Kane-Maguire, N. A. P.; Wright, L. L.; Guckert, J. A.; Tweet, W. S. *Inorg. Chem.* **1988**, *27*, 2905–2907.
- (24) Singh, P.; Richter, M. M. *Inorg. Chim. Acta* **2004**, *357*, 1589–1592.
- (25) Richter, M. M.; Bard, A. J.; Kim, W.; Schmehl, R. H. *Anal. Chem.* **1998**, *70*, 310–318.
- (26) Li, M.; Liu, J.; Zhao, C.; Sun, L. *J. Organomet. Chem.* **2006**, *691*, 4189–4195.
- (27) Molnar, S. M.; Jensen, G. E.; Vogler, L. M.; Jones, S. W.; Laverman, L.; Bridgewater, J. S.; Richter, M. M.; Brewer, K. J. *J. Photochem. Photobiol., A* **1994**, *80*, 315–322.
- (28) Nallas, G. N. A.; Jones, S. W.; Brewer, K. J. *Inorg. Chem.* **1996**, *35*, 6974–6980.
- (29) Elvington, M.; Brown, J.; Arachchige, S. M.; Brewer, K. J. *J. Am. Chem. Soc.* **2007**, *129*, 10644–10645.

(30) Holder, A. A.; Swavey, S.; Brewer, K. J. *Inorg. Chem.* **2004**, *43*, 303–308.

(31) Holder, A. A.; Zigler, D. F.; Tarrago-Trani, M. T.; Storrie, B.; Brewer, K. J. *Inorg. Chem.* **2007**, *46*, 4760–4762.

and the photocurrent detected with a high sensitive Keithley 6514 electrometer (Keithley, Cleveland, OH) was converted to a voltage before it was sent to the electrochemical workstation computer. ECL spectra were obtained by collecting the peak ECL intensity of the forward scan (~ 1.3 V vs Ag/Ag⁺ in MeCN) during the cyclic potential cycling at a scan rate of 50 mV/s with 24 pieces of interference filters (Intro, Inc. Socorro, NM) over a spectral range of 360 to 820 nm. These filters had an average half-peak width of 10 nm and a transmittance value of 50% at the specified wavelength.

Fluorescence spectra were recorded with a Spex Fluorolog 2 fluorimeter (Horiba Jobin Yvon Inc., NJ). UV-visible spectroscopic measurements were performed with a Shimadzu UV-2401 PC Spectrometer (Columbia, MD).

QCM experiments were performed on a QCM200 Quartz-crystal Microbalance Digital Controller with a QCM25 5 MHz Crystal Oscillator (Stanford Research Systems, Sunnyvale, CA). A 5 MHz polished gold/Cr-coated AT-cut quartz crystal, with diameters of 2.54 and 1.32 cm for the quartz and the gold, respectively, was used. Data obtained from electrochemical deposition of silver by potential-step experiments from a 5.0 mM AgNO₃ solution in 0.50 M HNO₃ were used to calibrate the QCM instrument,³⁴ resulting in a sensitivity factor of 51.7 Hz cm²/μg on the basis of the Sauerbrey equation.^{35–38}

Immobilization of ctDNA onto Au/QCM Electrodes. AT-cut 5 MHz quartz-gold electrodes were cleaned with freshly prepared piranha solution (98% H₂SO₄/30% H₂O₂, 70/30 in v/v) for ~ 10 min, followed by washing with copious amounts of distilled water and then ethanol. The piranha solution was handled carefully because of its ability to react violently with organic materials. The Au electrodes were subsequently dried in a stream of N₂ before being transferred into a 1.0 mM ethanol solution of 11-mercapto-1-undecanol for ~ 24 h. The resulting electrodes were washed with ethanol to remove excess 11-mercapto-1-undecanol and then air-dried. The electrodes were then placed into a 10 mL of 40 mM MES buffered solution (pH 6.4) containing 10 mM EDAC and 1.3 mM ctDNA per nucleotide determined spectrophotometrically by employing an extinction coefficient of 6600 M⁻¹ cm⁻¹ at 260 nm.³⁹ This mixture was kept at 4 °C for 72 h with addition of ~ 20 mg of EDAC into the solution every few hours. In this way, covalent immobilization of the ctDNA onto the thiol coated-Au/QCM electrode via phosphate ester formation from the condensation reaction between 5'-end of ctDNA and the hydroxyl group of 11-mercapto-1-undecanol can be realized.^{40,41} The obtained electrodes were cleaned with 0.20 M Tris-HCl buffer (pH 7.4) and

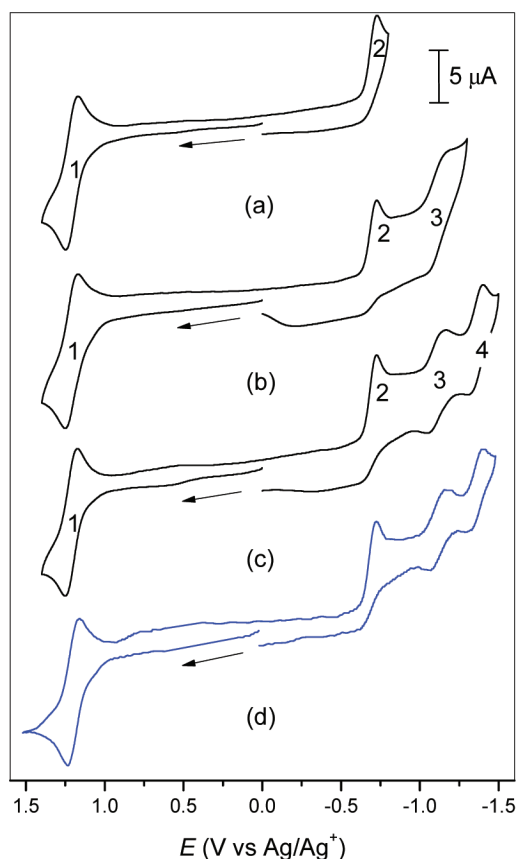


Figure 2. Cyclic voltammograms obtained from (a)–(c) 1.0 mM [((phen)₂Ru(dpp))₂RhCl₂](PF₆)₅ at various negative potential scanning limits and (d) 1.0 mM [((bpy)₂Ru(dpp))₂RhCl₂](PF₆)₅ in MeCN containing 0.10 M TBAP at a 2 mm Pt electrode with a scan rate of 50 mV/s.

distilled water, and then kept in 0.20 M Tris buffer-HCl (pH 7.4) at 4 °C until further use.

ctDNA-[(phen)₂Ru(dpp))₂RhCl₂]⁵⁺ Binding Constant Measurements. A QCM flow cell (Stanford Research Systems, Sunnyvale, CA) with above-mentioned ctDNA immobilized Au/QCM electrode was connected to a peristaltic pump (VWR International) and used for the ctDNA-[(phen)₂Ru(dpp))₂RhCl₂]⁵⁺ binding constant measurements. To eliminate the temperature effect on the frequency change of the QCM, the experiment was performed in a small constant temperature room of 25.00 ± 0.01 °C, and the flow cell, as well as the buffer solution (10.00 mL of 0.20 M Tris-HCl, pH 7.4), was kept in a thermo-insulating foam box on an anti-vibration pad. The instrument was pumped with the buffer at a flow rate of 0.44 mL/min until the frequency change of less than 0.1 Hz over 10 min was reached. This was followed by adding microliter levels of 1.00 mM [((phen)₂Ru(dpp))₂RhCl₂](PF₆)₅ in 0.20 M Tris-HCl (pH 7.4) to the buffer solution at various time intervals, and the corresponding frequency change was recorded.

RESULTS AND DISCUSSION

Cyclic Voltammetry of [((phen)₂Ru(dpp))₂RhCl₂]⁵⁺ Complex. Figures 2a–c show the cyclic voltammograms of 1.0 mM [((phen)₂Ru(dpp))₂RhCl₂](PF₆)₅ in MeCN containing 0.10 M

(41) Naylor, R.; Gilham, P. T. *Biochemistry* **1966**, *5*, 2722–2728.

- (32) Rosado, D. J., Jr.; Miao, W.; Sun, Q.; Deng, Y. J. *Phys. Chem. B* **2006**, *110*, 15719–15723.
- (33) Miao, W.; Wang, S. In *Handbook of Chemiluminescent Methods in Oxidative Stress Assessment*; Popov, I., Lewin, G., Eds.; Transworld Research Network: Kerala, India, 2008; Chapter 4, pp 41–83.
- (34) Wang, S.; Neshkova, M. T.; Miao, W. *Electrochim. Acta* **2008**, *53*, 7661–7667.
- (35) Buttry, D. A.; Ward, M. D. In *Electroanal. Chem.*; Bard, A. J., Ed.; Marcel Dekker: New York, 1991; Vol. 17, pp1–85.
- (36) Buttry, D. A.; Ward, M. D. *Chem. Rev.* **1992**, *92*, 1355–1379.
- (37) Sauerbrey, G. Z. *Phys.* **1959**, *155*, 206–22.
- (38) Ward, M. D. In *Physical Electrochemistry*; Rubinstein, I., Ed.; Dekker: New York, 1995; pp 293–338.
- (39) *Analytical Molecular Biology: Quality and Validation*; Saunders, G. C.; Parkes, H. C., Eds.; Royal Society of Chemistry: London, 1999.
- (40) Tombelli, S.; Minunni, M.; Mascini, M. *Anal. Lett.* **2002**, *35*, 599–613.

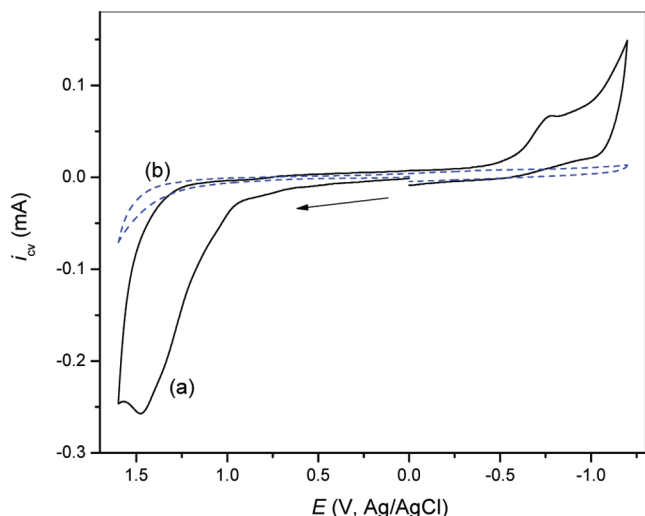


Figure 3. Cyclic voltammograms obtained from (a) 5.0 mM $[(\text{phen})_2\text{Ru}(\text{dpp})_2\text{RhCl}_2]\text{Cl}_5$ in 0.20 M Tris buffer (pH 7.4) at a 3 mm GC electrode with a scan rate of 50 mV/s, and (b) blank.

TBAP at various reduction potentials using a 2 mm Pt electrode at a scan rate of 50 mV/s. Only one reversible redox process (process 1) with $E_{1/2} = +1.21$ V versus Ag/Ag^+ that corresponds to the electron transfer of $\text{Ru}^{\text{II/III}}$ was observed, suggesting that the two Ru^{II} centers are chemically equivalent and largely electronically uncoupled.^{42,43} The irreversible reduction of process 2 at -0.73 V versus Ag/Ag^+ can be attributed to a two-electron transfer of Rh^{III} to Rh^{I} , which shows a slightly smaller peak current than that of process 1 as expected. Quasi-reversible process 3 ($E_{1/2} = -1.11$ V vs Ag/Ag^+ ; $\Delta E \approx 110$ mV) and process 4 ($E_{1/2} = -1.36$ V vs Ag/Ag^+ ; $\Delta E \approx 100$ mV) result from a one-electron transfer of the first ligand $\text{dpp}^{0/-}$ and the second $\text{dpp}^{0/-}$, respectively. This assignment is based on the ratio of peak current (Figure 2c, $i_{p2} \approx 2i_{p3} \approx 2i_{p4}$) as well as the comparison of the CVs between $[(\text{phen})_2\text{Ru}(\text{dpp})_2\text{RhCl}_2](\text{PF}_6)_5$ (Figure 2c) and its analogue $[(\text{bpy})_2\text{Ru}(\text{dpp})_2\text{RhCl}_2](\text{PF}_6)_5$ ³⁰ (where bpy = 2,2'-bipyridine, Figure 2d), where almost identical redox peak potentials are present for respective processes.

The CV of the complex (as chloride) in aqueous solution was conducted at a GC electrode with 0.20 M Tris buffer (pH 7.4) as the supporting electrolyte. In this way, a relatively wide potential window (GC vs Pt and Au) can be obtained, and the data obtained from the neutral pH media could be valuable for the production of intensive ECL in water.⁴⁴ Phosphate buffered solution was not chosen because the coordinated chloride ligand of the complex may slowly exchange with phosphate ions. As shown in Figure 3a, a large irreversible oxidation peak at +1.48 V versus Ag/AgCl on the forward scan and a relatively small, but broad irreversible reduction wave at -0.78 V versus Ag/AgCl on the reverse scan are observed. The former response must result from the oxidation of the two Ru^{II} species as discussed in MeCN, whereas the later wave appears to be a one-electron reduction of Rh^{III} to Rh^{II}

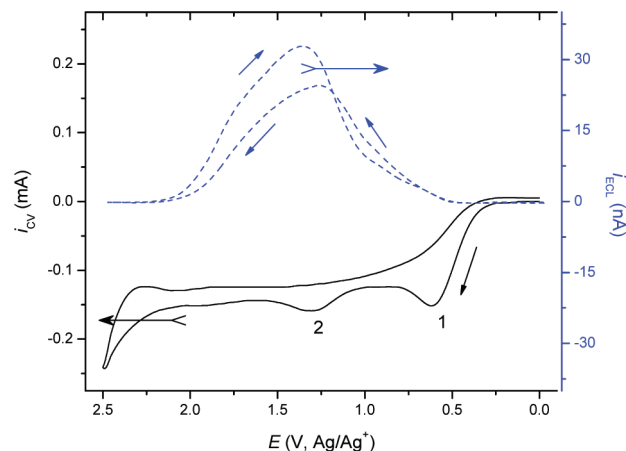
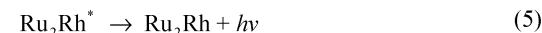
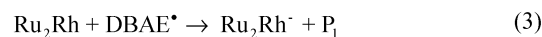


Figure 4. CV (solid line) and ECL (dashed line) responses of 0.10 mM $[(\text{phen})_2\text{Ru}(\text{dpp})_2\text{RhCl}_2](\text{PF}_6)_5$ with 0.10 M TBAP and 70 mM DBAE in MeCN at a 2 mm Pt electrode with a scan rate of 50 mV/s.

Scheme 1. Proposed ECL Mechanism of $[(\text{phen})_2\text{Ru}(\text{dpp})_2\text{RhCl}_2]^{5+}/\text{DBAE}$ System at Low Oxidation Potential Region in MeCN^a



^a Where DBAE = Bu_2NEtOH , $\text{DBAE}^{*+} = \text{Bu}_2\text{N}^{*+}\text{EtOH}$, $\text{DBAE}^* = \text{Bu}_2\text{NC}^*\text{HCH}_2\text{OH}$, $\text{P}_1 = \text{Bu}_2\text{N}^+ = \text{CHCH}_2\text{OH}$, $\text{Ru}_2\text{Rh} = [(\text{phen})_2\text{Ru}(\text{dpp})_2\text{RhCl}_2]^{5+}$.

because the ratio of integrated charge involved for the oxidation and reduction is close to 2:1.

ECL Behavior of $[(\text{phen})_2\text{Ru}(\text{dpp})_2\text{RhCl}_2]^{5+}$ Complex in MeCN and Aqueous Media. The oxidative-reduction type ECL⁴⁵ was used to investigate the ECL behavior of the complex in the presence of coreactant DBAE⁴⁶ and TPRA. Figure 4 shows CV (solid line) and ECL (dashed line) responses of 0.10 mM $[(\text{phen})_2\text{Ru}(\text{dpp})_2\text{RhCl}_2](\text{PF}_6)_5$ complex with 20.0 mM DBAE in MeCN containing 0.10 M TBAP at a Pt electrode. Peaks 1 and 2 on the CV result from the oxidation of DBAE (0.62 V vs Ag/Ag^+ , eq 1) and the oxidation of $[(\text{phen})_2\text{Ru}(\text{dpp})_2\text{RhCl}_2]^{5+}$ catalyzed by DBAE (1.30 V vs Ag/Ag^+). ECL profiles reveal that both forward and reverse scans generate broad ECL peaks around the oxidation peak potential of the emitter. Similar behavior was reported previously for the $\text{Ru}(\text{bpy})_3^{2+}/\text{TPRA}$ system in MeCN,^{47,48} although in the present case, noticeable ECL is produced even before the oxidation of $[(\text{phen})_2\text{Ru}(\text{dpp})_2\text{RhCl}_2]^{5+}$ species (i.e., in the potential range of 0.5 to

(42) Ammar, F.; Saveant, J. M. *J. Electroanal. Chem. Interfacial Electrochem.* **1973**, *47*, 215–21.

(43) Saveant, J.-M. *Elements of Molecular and Biomolecular Electrochemistry: An Electrochemical Approach to Electron Transfer Chemistry*; John Wiley & Sons, Inc.: Hoboken, NJ, 2006.

(44) Knight, A. W.; Greenway, G. M. *Analyst* **1996**, *121*, 101R–106R.

(45) Chang, M.-M.; Saji, T.; Bard, A. J. *J. Am. Chem. Soc.* **1977**, *99*, 5399–5403.

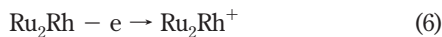
(46) Liu, X.; Shi, L.; Niu, W.; Li, H.; Xu, G. *Angew. Chem., Int. Ed.* **2007**, *46*, 421–424.

(47) Miao, W.; Bard, A. J. *Anal. Chem.* **2004**, *76*, 7109–7113.

(48) Miao, W.; Bard, A. J. *Anal. Chem.* **2004**, *76*, 5379–5386.

0.9 V vs Ag/Ag⁺). As shown in Scheme 1, this low potential ECL emission, as often seen from the Ru(bpy)₃²⁺/TPrA system in neutral media from GC and Au electrode,^{34,49–51} could be originated from the initial electrode oxidation of DBAE (eq 1), followed by a series of chemical reactions that lead to the formation of excited-state Ru₂Rh* species (eqs 2–4, where Ru₂Rh = [(phen)₂Ru(dpp)₂RhCl₂]⁵⁺, and Ru₂Rh[−] results from a one-electron reduction of the Rh center) and light emission (eq 5).

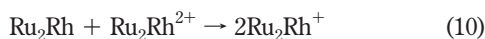
Similar to the Ru(bpy)₃²⁺/TPrA system, the ECL generation of the main waves in the Ru₂Rh/DBAE system should be also initiated by the electro-oxidation of the emitting complex. That is, upon the anodic potential scanning, DBAE is first oxidized and immediately deprotonated (eqs 1–2), followed by catalytic oxidations of Ru₂Rh with DBAE (eqs 6–8). Note that oxidations of Ru₂Rh shown in eqs 6 and 7 occur almost at the same electrode potential as revealed by CV (Figure 2).



Reduced Ru₂Rh species resulting from the reduction of the Rh center of the complex, Ru₂Rh[−] and Ru₂Rh^{2−}, are then formed via eqs 3 and 9.



The two-electron oxidized and reduced complexes could react with the parent species to produce the one-electron products in the course of diffusion toward the bulk solution (eqs 10–11).



In the co-presence of Ru₂Rh²⁺, Ru₂Rh⁺, Ru₂Rh[−], and Ru₂Rh^{2−}, the excited-state species, Ru₂Rh*, could be generated via the following four annihilation reactions (eqs 12–14), although a two-electron transfer to produce an excited state (eq 13) is unlikely.²⁵



Finally, the ECL is produced after the emission of light from Ru₂Rh* (eq 5). A previous ECL study on a bimetallic complex, [(bpy)₂Ru]₂(bphb)⁴⁺ (bphb = 1,4-bis(4'-methyl-2,2'-bipyridin-4-yl)benzene), has suggested that the one-electron annihilation reactions are the major ECL contributors.²⁵ Therefore, in the

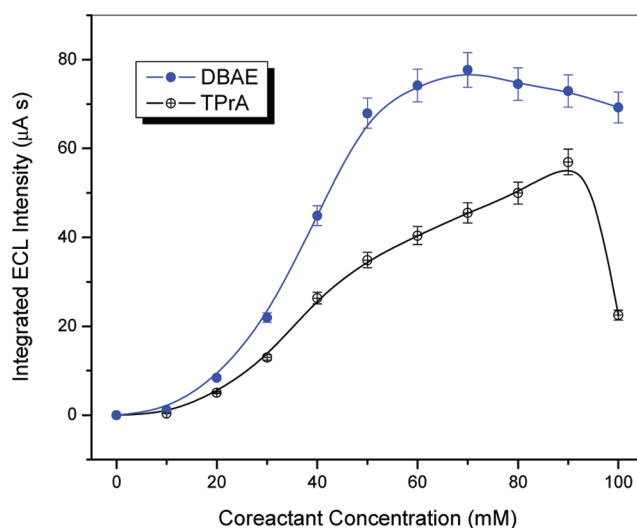


Figure 5. Effect of coreactant and its concentration on ECL intensity obtained from 0.10 mM [(phen)₂Ru(dpp)₂RhCl₂](PF₆)₅ containing 0.10 M TBAP with different concentrations of DBAE and TPrA in MeCN at a 2 mm Pt with a scan rate of 50 mV/s.

present case, contributions of eqs 12–13 and eq 15 to the overall emission process could be minor.

Very similar ECL profiles were observed when TPrA was used as the coreactant. However, as shown in Figure 5, much stronger ECL intensities are obtained from the DBAE system over an entire coreactant concentration range of 10 to 100 mM, in which the maximum ECL emissions at 70 mM of DBAE and 90 mM of TPrA at a Pt electrode in MeCN are evident. In addition, with respect to TPrA, DBAE produced much smaller background ECL signals in MeCN, resulting in a limit detection of 0.10 μM of the complex using 70 mM DBAE coreactant (eq 16).

$$\begin{aligned} \text{Integrated ECL intensity}(\mu\text{A s}) &= 0.901 + \\ &0.574 \times [\text{Ru}_2\text{Rh}](\mu\text{M}) \\ &([\text{Ru}_2\text{Rh}] \geq 0.10 \mu\text{M}, R^2 = 0.997) \quad (16) \end{aligned}$$

The effect of electrode material on the ECL generation was also studied. The relative integrated ECL intensity, obtained from a MeCN solution containing 0.10 M [(phen)₂Ru(dpp)₂RhCl₂](PF₆)₅–70 mM DBAE–0.10 M TBAP during the first potential cycle between 0 and 2.5 V versus Ag/Ag⁺ at a scan rate of 50 mV/s, at Pt, Au, and GC electrodes had a ratio of 100:100:30. The reason behind this still remains unclear.

Two ECL waves, located at +1.00 and +1.42 V versus Ag/AgCl, are present on the forward scan of the CV from the [(phen)₂Ru(dpp)₂RhCl₂]/Cl₅/TPrA system in 0.20 M Tris buffer (pH 7.4) at a GC electrode (Figure 6a). Under the same experimental conditions, the Ru(bpy)₃²⁺/TPrA system shows very similar ECL responses (Figure 6c), which suggests the same ECL mechanisms described previously⁴⁹ are probably operative for the two systems. In both cases, essentially the same CVs are obtained as displayed in Figure 6b because this process is predominately controlled by the TPrA oxidation (0.10 M), and the catalytic reactions of the ECL emitter (1.0 μM) with TPrA is negligible. When 1.0 μM Ru(bpy)₃²⁺/0.10 M TPrA is used as a reference ($\varphi_{\text{ECL}} = 1.0$), the 1.0 μM [(phen)₂Ru(dpp)₂RhCl₂]/Cl₅/0.10 M TPrA system showed an ECL efficiency of ~0.014 on the basis of the integrated ECL intensities. This is unexpected

(49) Miao, W.; Choi, J.-P.; Bard, A. J. *J. Am. Chem. Soc.* **2002**, *124*, 14478–14485.

(50) Zu, Y.; Li, F. *Anal. Chim. Acta* **2005**, *550*, 47–52.

(51) Zheng, H.; Zu, Y. *J. Phys. Chem. B* **2005**, *109*, 12049–12053.

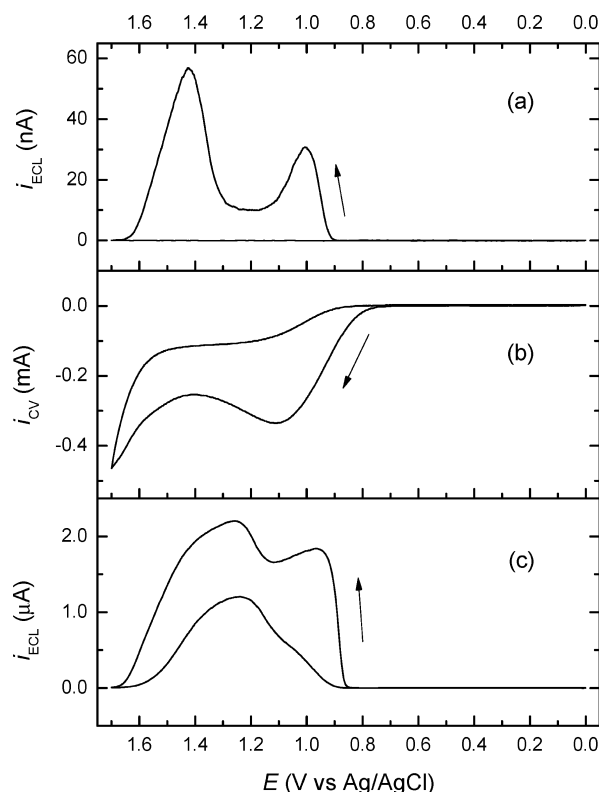


Figure 6. ECL responses of (a) $1.0 \mu\text{M}$ $[(\text{phen})_2\text{Ru}(\text{dpp})_2\text{RhCl}_2]\text{Cl}_5/0.10 \text{ M TPrA}$ and (c) $1.0 \mu\text{M}$ $\text{Ru}(\text{bpy})_3^{2+}/0.10 \text{ M TPrA}$ in 0.20 M Tris buffer (pH 7.4) at a 3 mm GC electrode at a scan rate of 50 mV/s . CV responses from both systems were essentially the same as displayed in (b).

because previously a few bimetallic Ru complexes have demonstrated several times increases in ECL efficiency as compared to the $\text{Ru}(\text{bpy})_3^{2+}$ standard.^{25,26} The complex Ru_2Rh in the present study has also two Ru^{II} centers but linked with a Rh-containing bridge (Figure 1). This Rh^{III} center can be reduced as described above by CV and can function as an electron acceptor. Therefore, the experimentally obtained low ECL efficiency from Ru_2Rh complex could be attributed to the efficient intramolecular electron-transfer quenching of Ru-based excited states by the Rh center.

A limit detection of 1.0 nM of $[(\text{phen})_2\text{Ru}(\text{dpp})_2\text{RhCl}_2]\text{Cl}_5$ was evaluated with 0.10 M TPrA as the ECL coreactant in 0.20 M Tris buffer neutral media at a GC electrode (eq 17). This limit of detection is about 100 and 1000 times lower than that obtained from UV–visible (see extinction coefficients of Ru_2Rh in SI section) and fluorescence spectroscopy, respectively.

$$\text{Log}[i_{\text{ECL}} (\mu\text{A s})] = 5.57 + 0.645 \times \text{Log}[\text{[Ru}_2\text{Rh]} (\text{M})]$$

$$([\text{Ru}_2\text{Rh}] \geq 1.0 \text{ nM}, R^2 = 0.999) \quad (17)$$

The ECL emission spectra recorded from the oxidative-reduction process of $[(\text{phen})_2\text{Ru}(\text{dpp})_2\text{RhCl}_2]^{5+}$ –DBAE in MeCN containing 0.10 M TBAP shows a broad emission band between 500 and 850 nm with a maximum at $\sim 640 \text{ nm}$ (Figure 7). Compared to the fluorescence that shows a broad spectrum at $\sim 695 \text{ nm}$, ECL spectra demonstrate a $\sim 55 \text{ nm}$ blue shift (Figure 7). This difference is unlikely due to possible problems associated with the ECL and fluorescence instruments (e.g., low resolution)

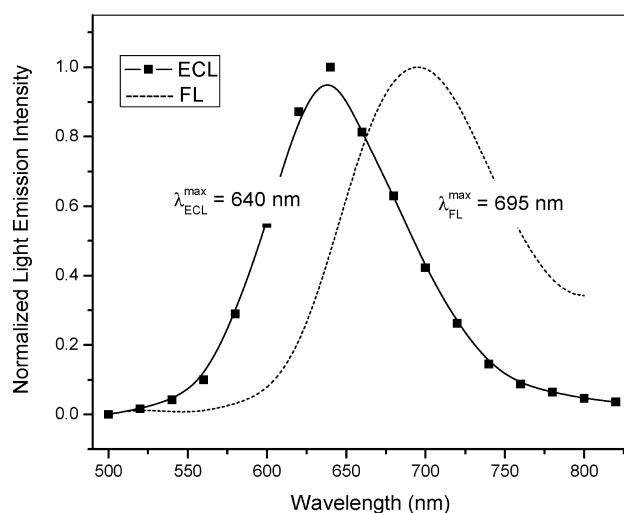


Figure 7. ECL emission (squared line) and fluorescence (dotted line) spectra of $[(\text{phen})_2\text{Ru}(\text{dpp})_2\text{RhCl}_2]^{5+}$ in MeCN. For ECL study a solution of 2.0 mM complex– 70 mM DBAE– 0.10 M TBAP in MeCN was used with a cyclic potential scanning between 0 and 2.50 V vs Ag/Ag^+ at a 2 mm Pt electrode at a scan rate of 50 mV/s . The fluorescence spectrum was produced with $0.10 \mu\text{M}$ of the complex in MeCN with an excitation wavelength of 400 nm .

where the spectra were collected because both instruments were precalibrated with the standard $\text{Ru}(\text{bpy})_3^{2+}/\text{TPrA}$ system. Such unusual blue shift behavior has been reported previously for three aryl-diamide bridged binuclear ruthenium (II) tris(bipyridine) complexes²⁶ as well as for a series of *N,N*-dimethylaminophenylethynylarenes,⁵² where a blue shift of ~ 24 – 65 nm ECL as compared to the fluorescence emissions were observed. The formation of the “H-type” excimers in the latter case was believed to be responsible for the blue shift. As a result, in our present study, the ECL emissive state may have a unique structure that is formed under the ECL experimental conditions (e.g., via ion annihilations) and is rather different from the photoluminescent state.

Interaction of $[(\text{phen})_2\text{Ru}(\text{dpp})_2\text{RhCl}_2]^{5+}$ Complex with ctDNA. QCM has been proven to be very sensitive in measuring nanogram-level mass changes at the surface of a QCM electrode in gas phase and in aqueous solution.^{36,53,54} For example, Okahata’s group^{55,56} has utilized QCM to detect various biomolecule interactions such as DNA–DNA hybridization,^{57,58} DNA–protein interactions,^{59,60} sugar–protein interactions,^{61–63} and protein–protein

- (52) Ho, T.-I.; Elangovan, A.; Hsu, H.-Y.; Yang, S.-W. *J. Phys. Chem. B* **2005**, *109*, 8626–8633.
- (53) Ricci, F.; Volpe, G.; Micheli, L.; Palleschi, G. *Anal. Chim. Acta* **2007**, *605*, 111–129.
- (54) *Piezoelectric Sensors in Springer Series on Chemical Sensors and Biosensors*; Steinem, C.; Janshoff, A., Eds.; Springer: New York, 2007.
- (55) Okahata, Y.; Mori, T.; Furusawa, H.; Nihira, T. In *Springer Series on Chemical Sensors and Biosensors*; Springer: New York, 2007; Vol. 5, pp 341–369.
- (56) Okahata, Y.; Niikura, K.; Furusawa, H.; Matsuno, H. *Anal. Sci.* **2000**, *16*, 1113–1119.
- (57) Okahata, Y.; Matsunobu, Y.; Ijiri, K.; Mukae, M.; Murakami, A.; Makino, K. *J. Am. Chem. Soc.* **1992**, *114*, 8299–300.
- (58) Caruso, F.; Rodda, E.; Furlong, D. N.; Niikura, K.; Okahata, Y. *Anal. Chem.* **1997**, *69*, 2043–2049.
- (59) Okahata, Y.; Niikura, K.; Sugiura, Y.; Sawada, M.; Morii, T. *Biochemistry* **1998**, *37*, 5666–5672.
- (60) Matsuno, H.; Niikura, K.; Okahata, Y. *Biochemistry* **2001**, *40*, 3615–3622.
- (61) Ebara, Y.; Okahata, Y. *Langmuir* **1993**, *9*, 574–576.
- (62) Ebara, Y.; Okahata, Y. *J. Am. Chem. Soc.* **1994**, *116*, 11209–11212.

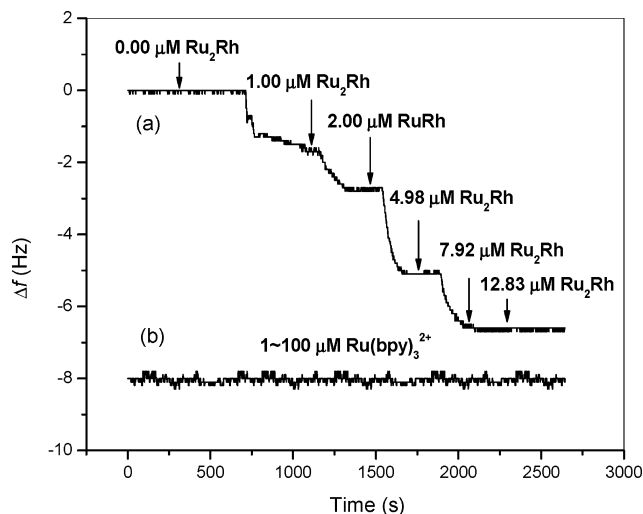


Figure 8. QCM frequency changes versus time for (a) intercalations of $[(\text{phen})_2\text{Ru}(\text{dpp})_2\text{RhCl}_2]^{5+}$ complex into ctDNA immobilized on a Au-coated QCM electrode in 0.20 M Tris buffer (pH 7.4) solution at 25.00 ± 0.01 °C, and (b) as (a) but the complex was replaced with $\text{Ru}(\text{bpy})_3^{2+}$. Concentrations are labeled as the final ones in the buffer and the flow rate of 0.44 mL/min was used.

interactions⁶⁴ in aqueous solution. One of the key principles for the above measurements is the Sauerbrey equation (eq 18),^{35–38} which indicates that the resonance frequency increases linearly upon the decrease of mass on a QCM electrode.

$$\Delta f = -C_f \times \Delta m \quad (18)$$

where Δf is the experimentally measured frequency shift caused by change of a mass per unit area, Δm , to the crystal surface, and C_f is the sensitivity factor which has a calibrated value of $51.7 \text{ Hz cm}^2/\mu\text{g}$ for our present QCM instrument.³⁴

In this study, the ctDNA- $[(\text{phen})_2\text{Ru}(\text{dpp})_2\text{RhCl}_2]^{5+}$ interactions in 0.20 M Tris-HCl buffer (pH 7.4) were monitored with QCM at a constant temperature of 25.00 ± 0.01 °C after additions of certain amounts of the complex into a flow QCM system that contains a ctDNA immobilized Au/QCM electrode. As shown in Figure 8a, with addition of the complex into the solution, the frequency drops accordingly, suggesting the intercalations of the complex into the DNA. This is confirmed by a control experiment (Figure 8b), where relatively high concentrations of $\text{Ru}(\text{bpy})_3^{2+}$ (1–100 μM) were added to a separate flow system with freshly prepared ctDNA-Au/QCM electrode. No frequency changes are observed as expected because $\text{Ru}(\text{bpy})_3^{2+}$ has been known to have no interactions with ctDNA.

An alternative plot of Figure 8a is shown in Figure 9a, where changes in mass (Δm) were calculated from eq 18, and the x-axis is the complex concentration in the flow system. Clearly, at the high concentration, intercalation of the complex into the DNA approaches a saturated-status. Assuming the interaction process meets the requirements of the Langmuir isotherm,^{65,66} the binding constant (i.e., equilibrium constant, K_b) can be expressed as



$$K_b = \frac{[\text{ctDNA-Ru}_2\text{Rh}]_{\text{QCM}}}{[\text{ctDNA}]_{\text{QCM}}[\text{Ru}_2\text{Rh}]} \quad (19b)$$

where $[\text{ctDNA}]_{\text{QCM}}$ and $[\text{Ru}_2\text{Rh}]$ represent the surface concentration of ctDNA on Au/QCM and the solution concentration of $[(\text{phen})_2\text{Ru}(\text{dpp})_2\text{RhCl}_2]^{5+}$ complex in the buffer, respectively. Thus, the relationship between the instant mass change (Δm), the maximum mass change (Δm_{max}), the solution concentration of the complex, and the binding constant (K_b) can be described as follows:

$$\Delta m = \Delta m_{\text{max}} \frac{[\text{Ru}_2\text{Rh}]K_b}{1 + K_b[\text{Ru}_2\text{Rh}]} \quad (20a)$$

Equation 20a can be rearranged to give eq 20b:

$$\frac{[\text{Ru}_2\text{Rh}]}{\Delta m} = \frac{1}{\Delta m_{\text{max}}K_b} + \frac{[\text{Ru}_2\text{Rh}]}{\Delta m_{\text{max}}} \quad (20b)$$

That is, $[\text{Ru}_2\text{Rh}]/\Delta m$ versus $[\text{Ru}_2\text{Rh}]$ should give a straight line, in which $1/(\Delta m_{\text{max}}K_b)$ will be the intercept and $1/(\Delta m_{\text{max}})$ will be the slope. Figure 9b depicts such a plot, which results in an intercept of $2.33 \times 10^{-2} \mu\text{M cm}^2 \text{ ng}^{-1}$ and a slope of $5.71 \times 10^{-3} \text{ cm}^2 \text{ ng}^{-1}$. Accordingly, $\Delta m_{\text{max}} = 175 \text{ ng cm}^{-2}$ and $K_b = 2.5 \times 10^5 \text{ M}^{-1}$ are obtained. This K_b value compares favorably with that of $K_{b(\text{EtBr})} = 1.2 \times 10^5 \text{ M}^{-1}$ for the binding of ethidium bromide (EtBr) to salmon testes DNA in a QCM experiment.^{59,67}

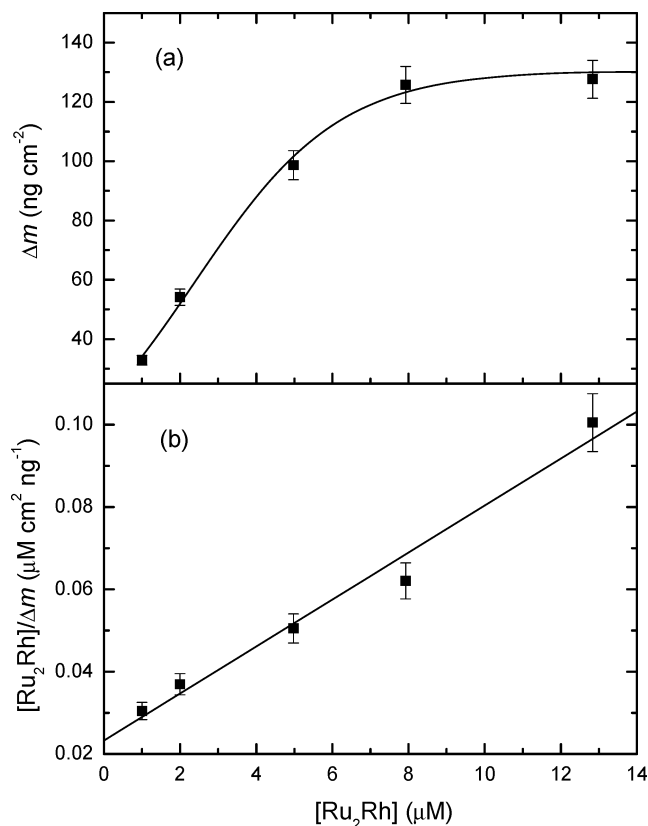


Figure 9. Langmuir isotherms obtained from the interactions between $[(\text{phen})_2\text{Ru}(\text{dpp})_2\text{RhCl}_2]^{5+}$ complex in 0.20 M Tris buffer (pH 7.4) and ctDNA immobilized on a Au-coated QCM electrode at 25.00 ± 0.01 °C. (a) Non-linear regression between Δm and $[\text{Ru}_2\text{Rh}]$, (b) linear regression between $[\text{Ru}_2\text{Rh}]/\Delta m$ and $[\text{Ru}_2\text{Rh}]$.

(63) Mori, T.; Sekine, Y.; Yamamoto, K.; Okahata, Y. *Chem. Commun.* **2004**, 2692–2693.

(64) Matsuno, H.; Furusawa, H.; Okahata, Y. *Chem.—Eur. J.* **2004**, *10*, 6172–6178.

(65) Langmuir, I. *J. Am. Chem. Soc.* **1916**, *38*, 2221–2295.

(66) Langmuir, I. *J. Am. Chem. Soc.* **1918**, *40*, 1361–1402.

$K_{b(\text{EtBr})}$ values of $2.6 \times 10^5 \text{ M}^{-1}$, $5 \times 10^5 \text{ M}^{-1}$, and $1.9 \times 10^5 \text{ M}^{-1}$ were also obtained with other techniques such as equilibrium dialysis,⁶⁸ surface plasmon resonance,⁶⁹ and UV–visible spectrophotometry,⁷⁰ respectively. The consistency of the QCM based binding constant $K_{b(\text{EtBr})}$ with those measured from other methods suggests that QCM could be a reliable technique for the measurement of binding constant for complex intercalations with double-stranded DNAs.

CONCLUSIONS

The electrochemical and electrogenerated chemiluminescent behavior of a mixed-metal supramolecular complex, $[(\text{phen})_2\text{Ru}(\text{dpp})_2\text{RhCl}_2]^{5+}$, was studied in MeCN and aqueous solutions. In MeCN, a reversible, overlapping redox process of $\text{Ru}^{\text{II/III}}$ and an irreversible reduction of $\text{Rh}^{\text{III/I}}$, followed by two quasi-reversible $\text{dpp}^{0/-}$ couples, were observed. In aqueous solution, however, the $\text{Ru}^{\text{II/III}}$ process became irreversible, and only one-electron transfer was involved in the reduction of Rh^{III} . ECL produced with both DBAE and TPrA coreactant suggested

that mechanisms similar to the $\text{Ru}(\text{bpy})_3^{2+}/\text{TPrA}$ system in respective solvent should be followed. About 55 nm blue shift of ECL to its fluorescence and 1.4% of ECL efficiency relative to the standard $\text{Ru}(\text{bpy})_3^{2+}/\text{TPrA}$ system were obtained. Interactions of the complex with ctDNA were monitored with a flow-cell based QCM in Tris buffer, which provided a binding constant of $2.5 \times 10^5 \text{ M}^{-1}$ on the basis of the Langmuir isotherm.

ACKNOWLEDGMENT

The abstract was presented at PITTCON 2008, March 2–7, 2008, New Orleans, LA. Financial support from USM startup (A.A.H. and W.J.M.), NSF-MRSEC (NSF-DMR 0213883), and NSF-IGERT (NSF-DGE 0333136) is gratefully acknowledged.

SUPPORTING INFORMATION AVAILABLE

Detailed procedures on the synthesis and characterization of $[(\text{phen})_2\text{Ru}(\text{dpp})_2\text{RhCl}_2]^{5+}$ complexes (as PF_6^- and Cl^- salts). This material is available free of charge via the Internet at <http://pubs.acs.org>.

- (67) Okahata, Y.; Ijio, K.; Matsuzaki, Y. *Langmuir* **1993**, *9*, 19–21.
 (68) Bresloff, J. L.; Crothers, D. M. *Biochemistry* **1981**, *20*, 3547–3553.
 (69) Tombelli, S.; Minunni, M.; Mascini, M. *Anal. Lett.* **2002**, *35*, 599–613.
 (70) Yielding, L. W.; Yielding, K. L.; Donoghue, J. E. *Biopolymers* **1984**, *23*, 83–110.

Received for review February 5, 2009. Accepted March 13, 2009.

AC900282Y